Table 1 Summary of gas gun impact and soft recovery experiments

Shot no.	Impactor velocity,[a] km/s	Initial impactor stress,[b] GPa	Initial impactor thickness, mm	Final impactor thickness,[c] mm	Buffer material	Initial buffer thickness, mm	Qualitative description of impactor fracture damage
178	0.890	0.94	9.11	10.05	Min-K 2000	3.93	Heavy
181	0.867	1.0	9.10	9.31	Polyrubber	4.33	Medium
182	0.878	1.1	8.86	8.80	Polyurethane foam	3.81	Medium
179	0.879	2.0	9.06	8.85	Silicone rubber	4.30	Medium to light
180	0.863	3.1	9.12	8.93	Nylon	3.77	Light
168[d]	0.861	3.1	9.04	8.80	Polyethylene	3.43	Light
186	0.882	3.6	9.04	8.71	Polyurethane	3.51	Medium to light
184	0.882	3.6	9.11	8.84	Butyl rubber	3.87	Medium to light
183	0.883	3.6	9.06	8.76	Polyester	3.83	Light
167	0.878	3.9	9.04	8.76	Neoprene	3.91	Medium to light
185	0.886	3.9	9.04	8.77	Micarta	3.74	Medium to light
187	0.887	5.0	9.05	8.94	Melmac	3.84	Medium

[a]The estimated uncertainty is 1%. [b]The estimated uncertainty is 5-10%. The Hugoniot of Armco iron[3,4] was used since the 1026 steel Hugoniot was not available. The buffer material Hugoniots were obtained from Refs. 3 and 5. Since the Hugoniot for butyl rubber was not available, the polyurethane Hugoniot was used for shot 184. [c]Measured in the central region of the specimens. [d]Obtained from Ref. 1.

the 1.0-GPa polyrubber and the 1.1-GPa polyurethane foam buffer shots. For these shots the damage was centered about 5-6 mm from the disk impact surface. Medium-to-light or light fracture damage occurred for the eight shots in the 2.0-3.9-GPa stress range. (The light fracture damage occurred for impact stresses of 3.1 and 3.6 GPa.) The fracture damage was centered 3-5 mm from the disk impact surface for these eight shots. Medium fracture damage occurred about 4 mm from the disk impact surface for the 5.0-GPa Melmac buffer shot.

These results indicate that the buffer materials with shock impedances that produced impact stresses of about 1 and 5 GPa caused a larger amount of impactor fracture damage than the buffer materials with impact stresses between 2 and 4 GPa. The lower shock impedance buffers have densities between 0.29 and 0.91 Mg/m^3; the higher shock impedance buffer has a density of 1.49 Mg/m^3. The lower shock impedance materials probably provide inadequate spall protection for the impactor disk from the composite specimen. (Complete spall separation of an impactor disk occurred after it impacted an unbuffered composite specimen at 0.88 km/s.[1]) The higher shock impedance buffer material probably provides adequate spall protection for the impactor disk from the composite specimen but likely causes impactor fracture damage itself.

Acknowledgments

The authors would like to acknowledge W. G. Soper, D. C. Smith, and W. E. Elliott Jr. for their support and helpful discussions during this work.

References

[1]Mock, W. Jr. and Holt, W.H., "Gas Gun Study of Polyethylene Buffers for Spall Fracture Reduction in Missile Materials," *Journal of Spacecraft and Rockets*, Vol. 18, Nov.-Dec. 1981, pp. 565-566.

[2]Mock, W. Jr. and Holt, W.H., "The NSWC Gas Gun Facility for Shock Effects in Materials," Naval Surface Weapons Center, Dahlgren, Va., NSWC/DL TR-3473, July 1976.

[3]Kohn, B.J., "Compilation of Hugoniot Equations of State," Air Force Weapons Laboratory, Kirtland Air Force Base, N.Mex., AFWL-TR-69-38, April 1969.

[4]Barker, L.M., "α-Phase Hugoniot of Iron," *Journal of Applied Physics*, Vol. 46, June 1975, pp. 2544-2547.

[5]McQueen, R.G., Marsh, S.P., Taylor, J.W., Fritz, J.N., and Carter, W.J., "The Equation of State of Solids from Shock Wave Studies," *High Velocity Impact Phenomena*, edited by R. Kinslow, Academic Press, New York, 1970, pp. 293-417.

AIAA 82-4180

Visible Emission from Space Shuttle Main Engine Mach Disks

J. Wormhoudt* and V. Yousefian*
Aerodyne Research, Inc., Bedford, Mass.

Introduction

THE visible radiation from rocket plumes, observed in the form of (relatively easily obtained) photographs, can provide information about plume properties. This has led to studies estimating the visible emission intensity from rocket plumes,[1] considering several common radiation mechanisms.[2] In the absence of afterburning, a major cause of radiating plume features is reheating of the exhaust gas as it traverses the normal shocks (or Mach disks) which occur in both under- and overexpanded jets.

A widely observed example of such features are the Mach disk heated regions, which appear as pale blue inverted cones behind each of the three Space Shuttle main engine (SSME) nozzles (Fig. 1). However, the SSME propellants are pure H_2 and O_2, and therefore none of the visible radiation mechanisms described in Ref. 2 can be responsible for the observed radiation. It is the purpose of this Note to suggest a source for this radiation. This source is a continuum emission peaking in the blue which has previously been observed only in laboratory experiments with hydrogen flames, whose origin is still not known with certainty.

Properties Behind the Mach Disk

The plume gas properties downstream of the Mach disk are required to predict the radiation. These properties can be estimated using the assumption of frozen chemical composition from the nozzle exit until reheating by the normal shock. This is a reasonable assumption since in this region the characteristic flow time is short with respect to the chemical relaxation time. With the frozen chemistry assumption, the flow is isentropic between the nozzle exit and the upstream

Received Nov. 4, 1981; revision received Feb. 26, 1982.

*Senior Research Scientist, Applied Sciences Division.

front of the normal shock. If the nozzle exit conditions and a parameter downstream of the shock (such as pressure) are specified, all the flow variables upstream and downstream of the shock can be determined as follows.

For a perfect gas, the standard isentropic and normal shock relations[3] could be used to predict the flow parameters across the shock. To take into account the changing properties of a real gas, the PACKAGE one-dimensional flow computer code[4] was modified to evaluate the gas properties on both sides of the normal shock. In addition to the frozen chemistry option used in this region, the PACKAGE code can predict concentrations of sets of species governed by chemical kinetics, or by chemical equilibrium based on the NASA Chemical Equilibrium Code.[5] Even in frozen flow, the species thermodynamic properties required during the calculation are evaluated using the JANNAF thermochemical tables.[6] Properties are evaluated using the three equations of conservation of mass, momentum, and energy across the normal shock[3]; equations for entropy and total enthalpy upstream of the shock (which remain equal to the known values at the nozzle exit); and equations of state upstream and downstream of the shock. These constitute seven equations for the seven unknowns of velocity, density, and temperature both upstream and downstream and pressure upstream of the shock.

The nozzle exit conditions are calculated given the characteristics of the SSME documented in Ref. 7. It operates with a mixture weight ratio (liquid oxygen/liquid hydrogen) of 6 to 1, a chamber pressure of about 3000 psia, and a nozzle expansion area ratio of 77.5 to 1, generating a vacuum thrust of 470,000 lbf. These values were used in equilibrium combustor and one-dimensional kinetic nozzle calculations using the PACKAGE code. Results of this calculation included a combustion chamber temperature of 3470 K, a nozzle exit pressure of 0.20 atm, and an exit temperature of 1315 K. With exit conditions known, the gas properties across the shock are calculated as outlined above by assuming that the pressure downstream of the first Mach disk has essentially recovered to 1 atm.

At the high temperature that results from shock heating, the mixture composition (frozen at the exit plane values) would not be in a state of chemical equilibrium. The final composition and temperature downstream of the shock is determined by a PACKAGE kinetic calculation. As the gas dissociates owing to the sudden heating, the temperature decreases, eventually reaching a steady state at about 3050 K. This is below the combustor value not only because of the gas velocity but because molecular dissociation (and hence radical production) can proceed further at 1 atm than at the more than 200 atm found in the combustor. The final steady-state species mole fractions behind the Mach disk are 0.55, 0.25, and 0.016 for H_2O, H_2, and O_2, respectively; 0.093, 0.071, and 0.016 for the radicals H, OH, and O, respectively; and 8.5×10^{-6} and 1.3×10^{-6} for HO_2 and H_2O_2, respectively. These concentrations are essentially equal to those at chemical equilibrium, and are achieved within 2 cm (35 μs) of passage through the normal shock.

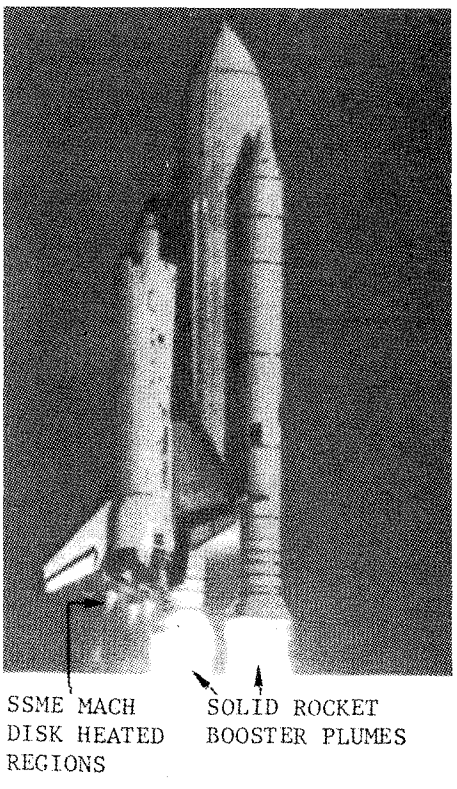

Fig. 1 First Space Shuttle launch (photo courtesy NASA).

Radiation Intensity Estimates

None of the molecules listed above are commonly thought of as visible radiators. However, chemiluminescent molecules formed from radical recombination can radiate even where no low-temperature absorption bands are observed. This can happen when the excited and ground state geometries differ, so that emission to highly excited vibrational states is favored, while absorption must proceed at much shorter wavelengths to high vibrational levels of the excited state.[8] Indeed, a blue chemiluminescent continuum emission from hydrogen/oxygen flames has been observed in several laboratory experiments,[9-11] yielding some evidence for the identity of the chemical process involved. However, these studies have generated conflicting results, which we now review.

The two emission mechanisms which have been proposed are

$$OH + OH \rightarrow H_2O_2 + h\nu \tag{1}$$

and

$$OH + H \rightarrow H_2O + h\nu \tag{2}$$

Diederichsen and Wolfhard[9] observed emission intensities at different pressures, and suggested that Eq. (1) was the more likely process because the mole fraction of OH is less sensitive to pressure than that of H, resulting in better agreement with the pressure dependence they observed. Padley[10] made observations in a series of flames of differing temperatures. Matching the temperature dependence of the emission intensity with that of measured H and OH radicals led him to the conclusion that Eq. (2) was the radiation mechanism. Most recently, Vanpee and Mainiero[11] observed the continuum spectra of a number of H_2/NO flames of different compositions, comparing the observed intensities with calculated equilibrium flame compositions. Their observations that the intensity decreased as the hydrogen content of the flame increased led them to abandon Eq. (2) as a possible mechanism. Furthermore, they found observed intensities to be roughly proportional to the square of the calculated OH concentration, in agreement with Eq. (1), and reported the observed photon emission rate at 375 nm as

$$I = 1.53\times10^{-21}[OH]^2 \text{ s}^{-1} \text{ nm}^{-1} \tag{3}$$

where [OH] denotes concentration in molecules per cubic centimeter.

It must be pointed out that the energy release from OH recombination is small enough to cast doubt on formation of H_2O_2 as an emission mechanism. In any case, Eq. (3), derived from a series of flames whose predicted equilibrium temperatures range from 3070 to 3130 K, is quite adequate to estimate emission from the present system no matter which radiation mechanism is correct. This is because in both the flames of Ref. 11 and the gas behind the Mach disk, the H and OH concentrations are within a factor of 2 of each other.

Evaluation of Eq. (3) and multiplication by the observed Mach disk radius of about 90 cm results in a maximum spectral radiance of 2×10^{-4} W cm^{-2} sr^{-1} nm^{-1}.

To see that this amount of radiation would be clearly visible against a sky background, we can compare it with an estimate of the sky radiance. The first Space Shuttle launch took place 45 min after sunrise, and the camera which took Fig. 1 was pointing west-northwest. For a comparable viewing geometry and the excellent visibility on the morning of launch, the sky radiance at 400 nm is no greater than 2×10^{-5} W cm^{-2} sr^{-1} nm^{-1} (Fig. 4-21 of Ref. 12), so the Mach disk emission predicted above would be quite bright against the sky. In fact, in the blue region, the shock emission is essentially equal to the intensity from the alumina particle loaded solid rocket booster plumes, calculated as described in Ref. 1. However, thermal emission intensity from alumina particles continues to increase into the near infrared, giving them a much higher total visible emission than the H_2/O_2 chemiluminescence. Finally, another candidate emission mechanism peaking in the blue was chemiluminescent CO_2 formed from recombining CO and O.[2] This would not only assume an unknown source of carbon (the SSME nozzles are designed to be reusable), but require a CO mole fraction of greater than 0.3.

Conclusions

The observation that a chemiluminescent process can outline the shock structure in a hydrogen/oxygen plume is a pleasant development allowing studies of the flowfields of these otherwise invisible plumes. The proposed mechanism and estimate presented here are more than enough to explain the observed intensity. With better understanding of the mechanism and the temperature dependence of the spectral intensity, this emission could become a quantitative diagnostic method, not only in H_2/O_2 exhaust plumes, but also in inert gas jets.

References

[1] Lyons, R.B., Wormhoudt, J., and Kolb, C.E., "Calculation of Visible Radiation From Missile Plumes," AIAA Paper 81-1111, June 1981.

[2] *JANNAF Handbook: Rocket Exhaust Plume Technology*, CPIA Publication 263, Chemical Propulsion Information Agency, Laurel, Md., 1980, Chap. 3.

[3] Liepmann, H.W. and Roshko, A., *Elements of Gasdynamics*, John Wiley and Sons, New York, 1957.

[4] Yousefian, V., Weinberg, M., and Haimes, R., "PACKAGE: A Computer Program for the Calculation of Partial Chemical Equilibrium/Partial Chemical Rate Controlled Composition of Multiphase Mixtures Under One Dimensional Steady Flow," Aerodyne Research, Inc., Rept. ARI-RR-177, Feb. 1980.

[5] Gordon, S. and McBride, B.J., "Computer Program for Calculation of Complex Chemical Equilibrium Composition, Rocket Performance, Incident and Reflected Shocks, and Chapman-Jouguet Detonations," NASA SP-2731, 1971.

[6] Chase, M.W., *JANAF Thermochemical Tables*, Dow Chemical Company, Midland, Mich., revised version, March 1979.

[7] "Liquid Propellant Engine Manual," CPIA Publication M5, Chemical Propulsion Information Agency, Laurel, Md., Unit No. 195, July 1979.

[8] Golde, M.F. and Thrush, B.A., "Afterglows," *Reports on the Progress of Physics*, Vol. 36, Oct. 1973, p. 1350.

[9] Diederichsen, J. and Wolfhard, H.G., "Spectrographic Examination of Gaseous Flames at High Pressure," *Proceedings of the Royal Society (London), Series A*, Vol. 236, April 1956, pp. 89-103.

[10] Padley, P.J., "The Origin of the Blue Continuum in the Hydrogen Flame," *Transactions of the Faraday Society*, Vol. 56, July 1960, pp. 449-454.

[11] Vanpee, M. and Mainiero, R.J., "The Spectral Distribution of the Blue Hydrogen Flame Continuum and Its Origin in Hydrogen-Nitric Oxide Flames," *Combustion and Flame*, Vol. 34, No. 3, April 1979, pp. 219-230.

[12] Wolfe, W.L. and Zissis, G.J., *The Infrared Handbook*, Environmental Research Institute of Michigan, Ann Arbor, Mich., 1978, pp. 4-31.